

## Analysis of the Biomass Behavior in the Combustion Process

HADEY Chaimaa<sup>1</sup>, ALLOUCH Malika<sup>1</sup>, ALAMI Mohammed<sup>1</sup>, LOULIDI Ilyass<sup>2</sup>, BOUKHELIFI Fatima<sup>2</sup>

<sup>1</sup> Engineering Sciences and Trades laboratory, ENSAM, University Moulay Ismail, Meknes, Morocco

<sup>2</sup> Equip Materials and Applied Catalysis Faculty of Science, University Moulay Ismail, Meknes, Morocco

### Abstract

Peanut shells (PS) and sugar canes (SC) constitute an attractive and an energetic biomass source in Morocco since they are renewable, abundant and available. This work seeks to study the thermal decomposition of these biomass samples and their derived solid biofuel under oxidative atmosphere, and it also attempts to determine their kinetic and thermodynamic combustion parameters. The solid biofuel samples were produced by slow pyrolysis at a temperature of 400°C. Based on the TGA results, the biomass combustion process goes through three stages which are the evaporation of moisture, devolatilization and char formation. For the biochar, it takes two steps that correspond to the evacuation of water and to the coal combustion. Kinetic parameters of each step are evaluated using Coats-Redfern method, and the thermodynamic parameters are calculated. The results have shown that biochar is less reactive than its original biomass, and that the biomass samples are the most reactive ones in the coal oxidation stage. We have also found that the biomass samples present a different combustion process. These results are useful for the configuration and the design of feasible systems for the conversion of this biomass into energy.

**Keywords** Biomass, Biochar, Combustion characteristics, kinetic parameters

Date of Submission: 04-11-2021

Date of acceptance: 18-11-2021

### I. INTRODUCTION

The growing demand for energy and the depletion of fossil fuels are the main reasons behind the considerable attention that is given to renewable energies [1]. Biomass is considered as an important source of energy, which presents several environmental advantages, thanks to its high abandonment, low price, renewability and carbon-neutrality [2]–[5]. It can also help reduce the emission of toxic gas such as NO<sub>x</sub> and SO<sub>x</sub> [6], [7].

Biomass is a difficult fuel to be exploited in its raw state because of several problems that arise such as: a quality diversity, low density and a calorific value. There are several ways to convert biomass into energy such as: the thermo-chemical and bio-chemical processes [8]. The thermo-chemical conversion technology is dominant because of its high efficiency conversion to gaseous, liquid and solid products under thermal conditions [9][10].

In this context, we are interested in thermochemical conversion and more precisely in slow pyrolysis which aims at maximizing the production of solid biofuel (biochar).

In fact, the biochar, resulting from the slow pyrolysis of biomass is a stable, homogeneous and a clean fuel. Generally, it has both low moisture and fixed carbon contents as well as a heating value that is higher than those of the raw biomass [11]. Biomass chars are found to have porous with highly disordered carbon structure and belong to the class of the most reactive carbon materials. The porosity within the chars causes more accessibility of the reactive gas to active sites resulting in an efficient combustion reactivity [12].

Kinetic and thermodynamic parameters determination seems necessary in order to properly characterize and understand the biomass samples combustion process and their biochar. Thermogravimetric analysis (TGA) is a common technique that is generally used to study the biomass combustion behavior and allow the kinetic parameters estimation, including activation energy ( $E_a$ ), reaction order and pre-exponential factor using the Coats-Redfern method.

Many researchers have used TGA to study the biomass pyrolysis process [6,8-12] or biomass

combustion process [13]–[15]. However, very few studies of the biomass with its biochar combustion process have been conducted. In this regards, this study aims at providing information on the combustion process of peanut shells, sugar canes and their derived biochar using the TGA technique. The objectives of our works are as follows: (a) the study of biomass and biochar combustion behavior, (b) determination of kinetic model and kinetic combustion parameters of the studied biofuel (c) evaluation of thermodynamic parameters.

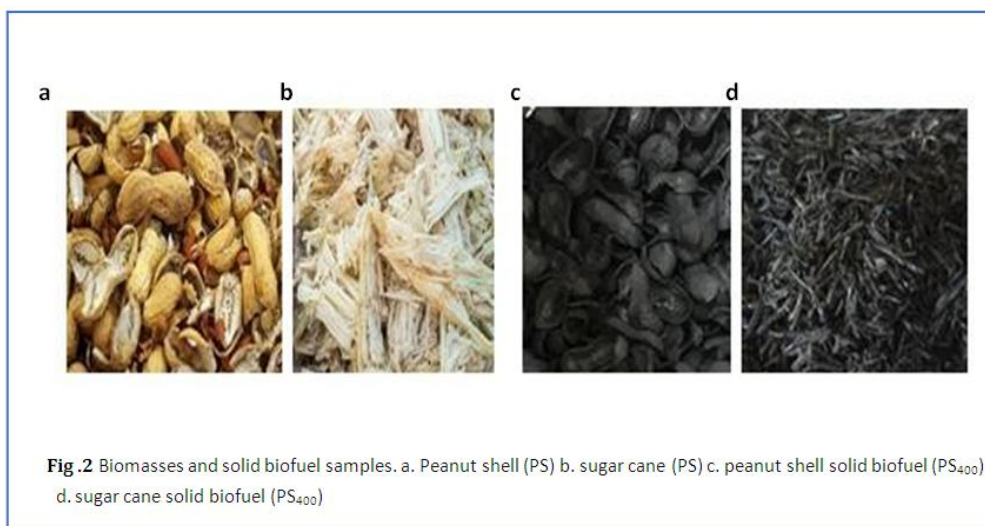
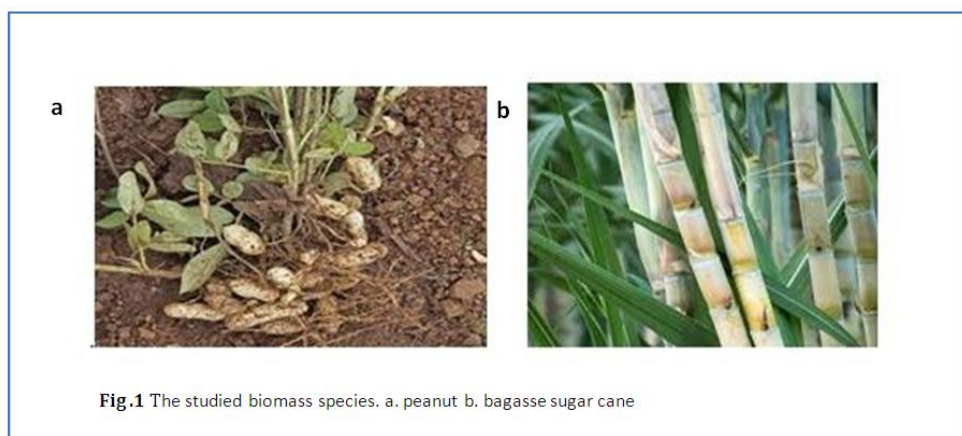
## II. MATERIALS AND METHODOLOGY

### Raw materials

The biomass of this study was the peanut shell and sugar cane produced in the region of Morocco (Fig.1). In the laboratory, the biomass was allowed to dry naturally at room temperature for one week. It was then subjected to oven drying at 105°C to constant weight and stored in a desiccator

### Solid biofuel Preparation

The solid biofuel (biochar) is obtained by slow pyrolysis of biomass samples in a muffle furnace under an inert atmosphere. The experiments were carried out at a temperature of 400°C for 2 h. (Fig.2) presents the obtained biochar. The biomass and the biochar samples are then crushed on a small scale to have small and more homogeneous samples. Finally, they are stored in a desiccator for ana



### Samples' Characterization

#### Constitutional and proximate analysis

Table 1 and 2 show the proximate and the constitutional analysis of the biomasses used in this study. Biomass samples' constitutional analysis is made according to Shiguang method [16]. Proximate analysis measurements are conducted using a thermogravimetric analysis [17].

**Table 1** Biomass samples' constituent analysis (%)

Samples	Extractible	Hemicellulose	Cellulose	Lignin
PS	4	62	22	12
SC	5	69	16	10

**Table 2** Biomass samples' proximate analysis (%)

Samples	Volatile matters	Ash	Fixed carbon
PS	82.00	3.34	14.66
SC	88.01	1.99	10.00

*Infrared spectroscopy*

Fourier transform infrared spectroscopy (FTIR) analysis is performed using the FTIR spectrometer to identify the functional groups that are present in the samples. The analysis is carried out by preparing pastilles with KBr in ratios of 1: 100. The infrared scanning range was 500 to 4000 cm<sup>-1</sup> with a resolution of 4 cm<sup>-1</sup>.

**Thermogravimetric analysis**

The thermal degradation behavior of the biomass samples and their biochar IS determined using a Shimadzu DTG 60 ATG thermogravimetric analyzer. The combustion experiments ARE carried out in air, UNDER a heating rate of 5°C / min from ambient temperature to a temperature of 1000°C. Slow heating rate IS selected to allow studying the thermal behavior under certain conditions in which the transport processes do not hide the study of the chemistry effects[18].

**Kinetic analysis**

The kinetics of decomposition reactions are largely described by Arrhenius's Law which provides information on thereaction rate.

$$d\alpha = K(T) \cdot f(\alpha) \quad (1)$$

Where  $\alpha = \frac{m_0 - m}{m_0 - m_f}$ ,  $m_0$ ,  $m$  and  $m_f$  are successively the initial mass, the current mass and the final mass. Generally,

K (T) has the form of Arrhenius's law:

$$K(T) = A \exp\left(-\frac{Ea}{RT}\right) \quad (2)$$

With A: Pre-exponential factor or frequency factor,

E: activation energy,

R: the universal constant of gases

Since the heating rate b is constant, it can be expressed by  $\beta = \frac{dT}{dt}$ .

Thus, combining Eq. (1) and Eq. (2) gives:

$$\frac{d\alpha}{dT} = \frac{A}{\beta} \exp\left(-\frac{Ea}{RT}\right) \cdot f(\alpha) \quad (3)$$

The g(x) is the integral function of conversion. By integrating eq.3, we obtain:

$$g(\alpha) = \int_0^\alpha \frac{d\alpha}{f(\alpha)} = \frac{A}{R} \int_{T_0}^T \exp\left(-\frac{Ea}{RT}\right) dT \quad (4)$$

The expression,  $\int_{T_0}^T \exp\left(-\frac{Ea}{RT}\right) dT$  has no exact analytical solution in that the resolution of the integral is difficult

,and it is only done by numerical solution or using the approximation proposed by Coats and Redfern[9]. We obtain :

$$\frac{A}{\beta} \int_{T_0}^T \exp\left(-\frac{Ea}{RT}\right) dT = \frac{ART^2}{\beta Ea} \left(1 - \frac{2RT}{Ea}\right) \exp\left(-\frac{Ea}{RT}\right) \quad (5)$$

After dividing T2 and introducing the logarithm, the equation (5) becomes:

$$\ln \left( \frac{g(\alpha)}{T^2} \right) = \ln \frac{AR}{\beta Ea} \left( 1 - \frac{2RT}{Ea} \right) - \frac{Ea}{RT} \quad (6)$$

(6)

The term 2RTE is much less than 1 for the thermal decomposition of lignocellulosic material [19], so it can be neglected. Eq. 3 can be written in the following form:

$$\ln \frac{g(\alpha)}{T^2} = \ln \frac{AR}{\beta Ea} - \frac{Ea}{RT} \quad (7)$$

The activation energy and the pre-exponential factor can be obtained from the slope  $-\frac{Ea}{R}$  and the ordinate at the origin of the line of the curve  $\ln \frac{g(\alpha)}{T^2}$  as a function of  $\frac{1}{T}$ . We HAVE adopted ten kinetic models to study the thermal decomposition of samples (Table 3)

**Table 3** Reaction mechanism, model names with their f(α) and g(α)

Mechanism	Symbols	F(α)	G(α)
Chemical Reaction-first order [20]	F1	1-α	-ln(1-α)
Chemical Reaction-second order	F2	(1-α) <sup>2</sup>	(1-α) <sup>-1-1</sup>
Chemical Reaction-third order	F3	(1-α) <sup>3</sup>	((1-α) <sup>-2-1</sup> )/2
Diffusion One Way transport[19]	D1	1/2α	α <sup>2</sup>
Diffusion Two Way transport	D2	(-ln(1-α)) <sup>-1</sup>	α+(1-α)ln(1-α)
Diffusion Three Way transport	D3	(2/3(1-α) <sup>2/3</sup> /1-(1-α) <sup>1/3</sup>	(1-(1-α) <sup>1/3</sup> ) <sup>2</sup>
Ginstling, Brounshtein equation	D4	(2/3)(1-α) <sup>1/3</sup> /1-(1-α) <sup>1/3</sup>	1-2 α/3-(1-α) <sup>2/3</sup>
Zhuravlev, Lesokhin, Tempelman equation	D5	(2/3)(1-α) <sup>5/3</sup> /1-(1-α) <sup>1/3</sup>	((1-α) <sup>-1/3-1</sup> ) <sup>2</sup>
Phase Boundary Controlled[19] R2 – contracting cylinder	R2	2(1-α) <sup>1/2</sup>	1-(1-α) <sup>1/3</sup>
Phase Boundary Controlled R3 – Contracting Sphere	R3	3(1-α) <sup>2/3</sup>	1(1-α) <sup>2/3</sup>

### Thermodynamic parameters Calculation

Thermodynamic data determination is also important in defining the process feasibility and in performing the energy calculations [21]. From the thermogravimetric analysis, we obtain the thermodynamic parameters such as the change of enthalpy H, entropy S, and the Gibbs free energy variation G. These parameters were calculated by the following equations[22]:

$$\Delta H = Ea - RT \quad (8)$$

$$\Delta G = Ea + RT \ln \frac{K_B T}{hA} \quad (9)$$

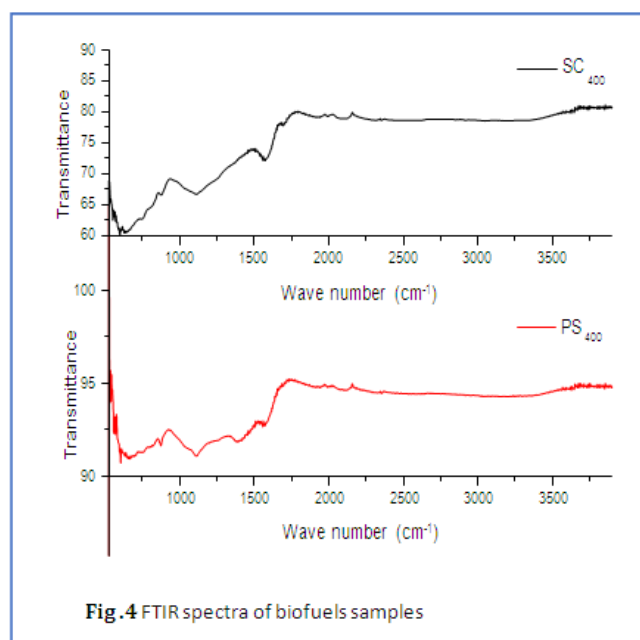
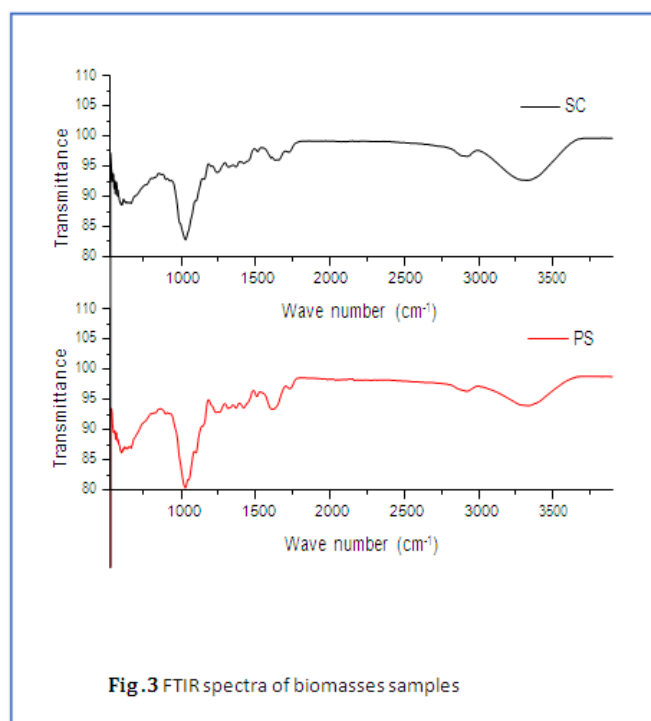
$$\Delta S = \frac{\Delta H - \Delta G}{Tm} \quad (10)$$

KB and h are respectively the Boltzman and Planck constant

### III. RESULTS AND DISCUSSION

#### Infrared spectroscopy

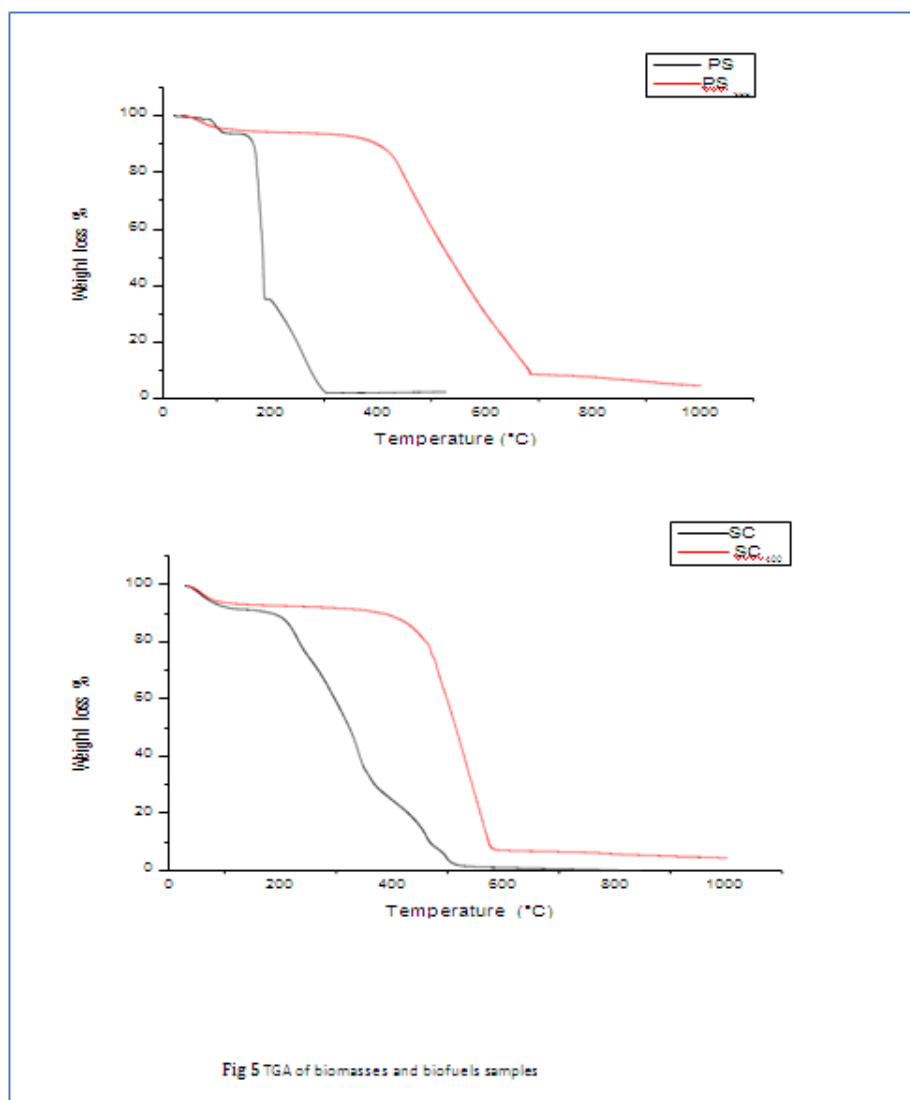
Fourier transform infrared spectroscopy (FTIR) is used to study the functional groups present in any substance. (Fig.3) shows the spectra with very tense and varied peaks of biomass and biochar samples. We HAVE found that all biomass samples have similar aromatic and aliphatic functional groups that come from the three main constituents of the studied wastes namely cellulose, hemicellulose and lignin. Indeed, these three components are mainly composed of alkenes, esters, ketones, aromatic rings and Alcohol with different functional groups containing oxygen such as O-H(3400- 3200 $\text{cm}^{-1}$ ) C=O(1765-1715  $\text{cm}^{-1}$ ), C-O-C(1270 $\text{cm}^{-1}$ ), and C-O-H(1050 $\text{cm}^{-1}$ ) [18,[23].



Comparing the spectra of the biomass samples with the biochar samples, we HAVE observed a decrease in the intensity of the C-O-C peaks and the alcohol -OH (1160-1030  $\text{cm}^{-1}$ ). The biochar spectra HAS shown that pyrolysis at 400 ° C caused degradation of cellulose and hemicellulose. The FTIR spectra of the biomasses HAS ALSO revealed the presence of a broad peak at 3280  $\text{cm}^{-1}$  related to the OH valency variation of the hydroxyl groups and a peak at 2926 related to the aliphatic CH elongation vibration in that both peaks have been completely removed from the biochar spectrum. Similarly, the peak corresponding to the variation of the aromatic C = C valence (1620  $\text{cm}^{-1}$ ) HAS disappeared from the biochar spectra to decompose into volatile matter during the pyrolysis. There is a lack of peaks between 700 and 900  $\text{cm}^{-1}$  on the biomass spectrum illustrating that the pyrolysis of biomass is a transient process from the aliphatic composition to the aromatic composition [24].

### Samples' thermal degradation behavior

Figure 5 and 6 show the TG and DTG curves of peanut shell, sugar cane and their biochar. The biomass samples' combustion HAS TAKEN place in three main stages. While the first step happens from 20 to 110°C corresponding to the loss of water and the evacuation of light molecules, the second step is attributed to the volatile compounds' evacuation generated by the hemicellulose and cellulose' decomposition. For the third stage, it is concerned with the decomposition of lignin and the combustion of coal. Devolatilization has two peaks in that the first one is due to the decomposition of hemicellulose, and the second is caused by the cellulose's decomposition [5,13]. Peanut shell and sugar cane Biochar combustion occurs in two main stages. For the first stage, it is between 30 and 130 ° C corresponding to the evacuation of water. As for the second one, it is characterized by a large peak at 505° C which is attributed to the combustion of coal. Volatilization peaks do not appear on the DTG curve because most of the volatiles were released during slow pyrolysis.



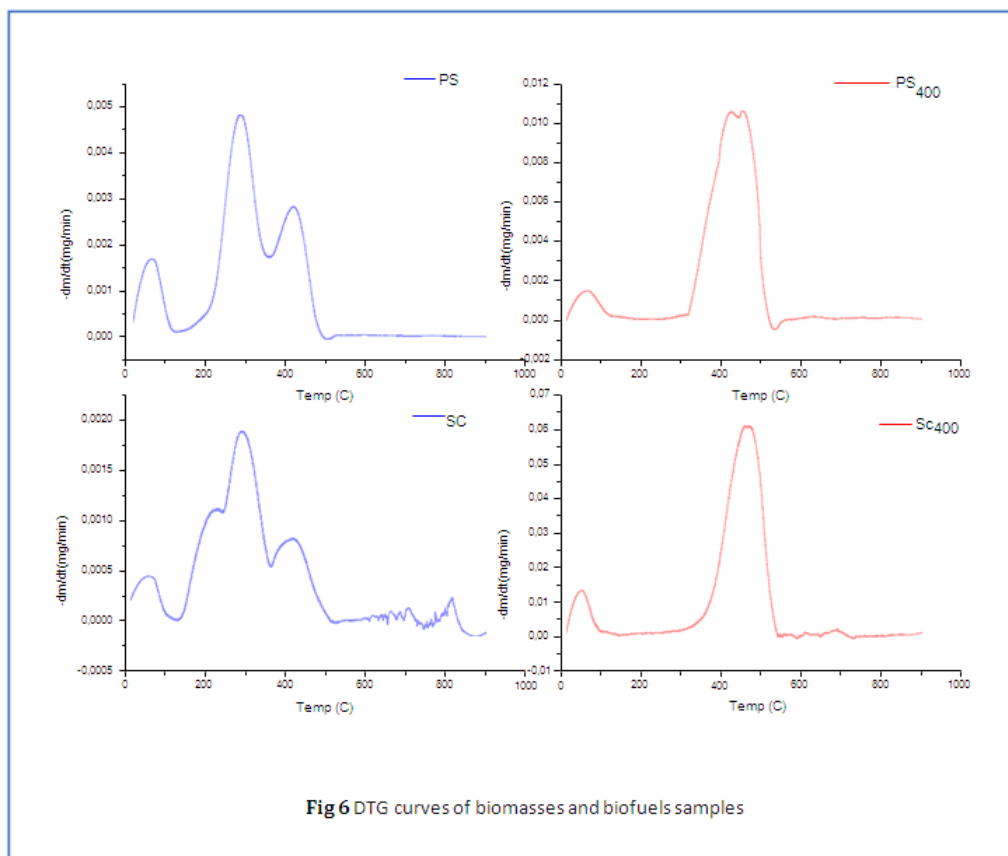


Fig 6 DTG curves of biomasses and biofuels samples

**Kinetic behavior**

The activation energy and the frequency factor THAT ARE calculated from the slope of the Coats-Redfern plots are presented in Table (4 and 5). The mass loss kinetics for the samples studied IS determined according to the highest correlation coefficient by the model representing the form of g(a) (Table 3). Based on coefficients correlation value (R2), we HAVE chosen the appropriate models. Indeed, the chosen models present an R2 between 0.89 and 0.99, which shows that the mechanisms are justified. Table 4 and 5 demonstrate the kinetic parameters (Ea, A) of combustionstep of the raw biomass and its derived biochar.

**Table 4** Biomasses samples’ Kinetic parameters using various reaction models

	T (C°)	Model	Ea (Kj/mol)	A(min <sup>-1</sup> )	R2
PS	216-361	D3	16.45	2062779.34	0.99
	361-500	D3	9.63	52432.62	0.95
SC	172-365	F3	17.37	3148077.45	0.98
	365-500	D3	10.64	82745.62	0.99

**Table 5** Biofuels samples’ Kinetic parameters using various reaction models

	T(C°)	Model	Ea (KJ/mol)	A(min <sup>-1</sup> )	R2
PS400	308-530	F2	47.22	779427226	0.89
SC400	386-550	F3	92.68	2.8710 <sup>-13</sup>	0.97

According to the results shown in table 4, the kinetic parameters characterizing the process of combustion of biomass samples differ from one stage to another and from one sample to another. The combustion of two biomass samples, which occurred in two stages, IS better characterized by a diffusion control mechanism for the first zone of PS ,and isbetter described by the third order chemical reaction model F3 for the first zone of SC. The second zone IS best characterized by a diffusion controlled mechanism for the two

samples. This suggests that the diffusion of oxygen to the char particle and of volatiles substances controls the combustion process from ignition to burnout.

By calculating the kinetic parameters using the models that have given the best correlation, peanut shell HAS an apparent activation energy of 16.45 KJ/mol for the first zone and 9.63 KJ/mol for the second one, . For sugar cane, it presents a value of 17.37 KJ/mol and 10.64 KJ/mol respectively for both the first and the second zone. Comparing this kinetic parameters, we HAVE found that the activation energy of the two samples' combustion steps is classified as follows:  $E$  (zone 1)  $>$   $E$  (zone 2). This means that the char oxidation stage requires less energy to react than that required in volatile matter release stage.

The combustion of Biochar PS400 and SC400 IS controlled by reaction kinetics particularly THE second and third order mechanism. The two biochar samples presents activation energies of 47.22 kJ/mol and 92.86 KJ/ mol respectively for PS400 and SC400. In this respect, this value HAS shown that bio char HAS had a high activation energy than their parent biomasses. In fact, the combustibility is not only affected by activation energy, but it is also influenced by the pre-exponential factor [25]. The same classification of activation energies is obtained for the pre-exponential factors. The biomass HAS a pre-exponential factor of  $2062779.34 \text{ min}^{-1}$  and  $3148077.45 \text{ min}^{-1}$  for the first zone and  $52432.62 \text{ min}^{-1}$  and  $82745.62 \text{ min}^{-1}$  for the second zone successively for PS and SC. While the biochar samples presented a pre-exponential factor of  $779427226 \text{ min}^{-1}$  and  $2.8710 \times 10^{13} \text{ min}^{-1}$  respectively for PS400 and SC400, the pre-exponential factor reflects the number of collisions between activated molecules that is called an effective collision.

The peanut shell's raw biomass and biochar samples are more reactive and have higher flammability in comparison to the raw biomass and biochar samples of sugar cane since they presented little activation energy whose reactions with high activity energy required high temperature and longer reaction time.

### Thermodynamic Parameters

The change in  $\Delta H$  has shown the differences in the energy existing between the activated complex and the reagents agreed with the activation energies [23,22]. If this difference is small, then, the formation of activated complex is favored because of the potential energy barrier inferiorit [26]. The positive  $\Delta H$  has shown that an external source of energy is required to raise the energy level of the reagents. In addition to that, higher values of the enthalpy indicate a less reactive system. Based on table 6 and 7, lower heat energies is required for the biomass, mainly in the second zone, than for the biochar to oxidate the reagents [27]. Thus, the formation of activated complex is more favored in biochar.

The Gibbs free energy  $\Delta G$  reveals an increase in the the total energy approach of the reagents and the formation of the activated complex. This change is due to MODIFICATION OF THE change  $\Delta S$  and a comprehensive evaluation of the heat flow  $\Delta H$  IN WHICH a higher value of  $\Delta G$  represents a lower favorability of reaction. The biomass has a  $\Delta G$  of 86.39 and 88.07 for the first zone and 114.44 and 111.64 for the second zone respectively for PS0 and SC0, while the biochar has values that are higher 156.91 for PS400 and 207.76 for SC400 and has the lowest energy barrier and absorbs the least amount of heat during combustion. According to the obtained results in table 6 and 7, we notice that  $\Delta S$  has a negative value for ALL samples which indicates that the disorder of the system is decreased and which henceforth confirms the disorder of products resulting resulted from the bond dissociation that is lower than the initial reactants.

**Table 6** Thermodynamic parameter estimation of biomasses samples

Samples	Ea(KJ/mol)	A	H	G	S
PS	16.45	2062779.34	14.07	86.39	-0.252
	9.63	52432.62	7.15	114.44	-0.256
SC	17.37	3148077.45	14.96	88.07	-0.252
	10.64	82745.62	6.20	111.64	-0.255

**Table 7** Thermodynamic parameter estimation of biofuels samples

Samples	Ea(KJ/mol)	A	H	G	S
PS400	47.22	779427226	43.54	156.91	-0.256
SC400	92.68	2.8710*	88.83	207.76	-0.256

## IV. CONCLUSION

The combustion process of peanut shells, sugar cane and their derived biochar have been studied at a heating rate of 5°C using a thermogravimetric analysis. The results have shown that:

□ The biomass samples (PS and SC) combustion is represented by three steps in which the first step



corresponds to the evaporation of moisture, the second to the devolatilization and the third one matches the char formation.

□ Biochar combustion occurs in two main stages attributed to the evacuation of water and to the combustion of coal.

□ The biomass kinetic study shows that the first zone of combustion is best fitted by diffusion-controlled mechanisms for peanut shell, and by chemical reaction-controlled mechanisms for sugar cane. As far as the second zone is concerned, the two biomass samples are best fitted by diffusion-controlled mechanism.

□ The thermodynamic parameters for the reagent active complex formation during combustion are calculated. The high values of  $\Delta H$  and  $\Delta G$  have shown that biochar is less reactive than its original biomass. Also, the  $\Delta S$  values of all biomass samples and biochar indicates that the disorder of the system has decreased. The obtained kinetic and thermodynamic parameters are useful in the conception of combustion reactors of peanut shell, sugar cane and their biochar.

Abbreviations			
<b>PS</b>	Peanut shell	<b>da/dt</b>	Conversion rate % min <sup>-1</sup>
<b>SC</b>	Sugar cane	<b>a</b>	Conversion degree %
<b>PS400</b>	peanut shell pyrolyzed at 400 °C	<b>β</b>	Heating rate K.min <sup>-1</sup>
<b>SC400</b>	Sugar cane pyrolyzed at 400 °C	<b>R<sup>2</sup></b>	Correlation coefficient
<b>TGA</b>	Thermogravimetric analysis	<b>g(a)</b>	Integral kinetic model
<b>DTG</b>	Differential Thermogravimetric	<b>F(a)</b>	Differential kinetic model
<b>FTIR</b>	Fourier transform infrared spectroscopy	<b>ΔG</b>	Free Gibbs energy KJ.mol <sup>-1</sup>
<b>T</b>	Temperature	<b>ΔS</b>	Entropy J.mol <sup>-1</sup>
<b>t</b>	Time	<b>ΔH</b>	Enthalpy KJ.mol <sup>-1</sup>
<b>K(t)</b>	Reaction rate constant	<b>T<sub>m</sub></b>	DTG max peak temperature K
<b>E<sub>a</sub></b>	Activation energy KJ.mol <sup>-1</sup>	<b>K<sub>h</sub></b>	Boltzmann constant (1.381*10 <sup>-23</sup> )J.K <sup>-1</sup>
<b>A</b>	Pré-exponential factor s <sup>-1</sup>	<b>H<sub>A</sub></b>	Plank constant (6.626*10 <sup>-34</sup> )J.s
<b>R</b>	Universal gaz constant		

### REFERENCES:

- [1]. X. Kai, T. Yang, Y. Huang, Y. Sun, Y. He, and R. Li, "The effect of biomass components on the co- combustion characteristics of biomass with coal," Proc. 2011 2nd Int. Conf. Digit. Manuf. Autom. ICDMA2011, pp. 1274–1278, 2011.
- [2]. J. Krasulina, H. Luik, V. Palu, and H. Tamvelius, "Thermochemical co-liquefaction of Estonian kukersite oil shale with peat and pine bark," Oil Shale, vol. 29, no. 3, pp. 222–236, 2012.
- [3]. P. McKendry, "Energy production from biomass (Part 1): Overview of biomass.," Bioresour. Technol., vol. 83, no. 1, pp. 37–46, 2002.
- [4]. A. Saraeian, M. W. Nolte, and B. H. Shanks, "Deoxygenation of biomass pyrolysis vapors: Improving clarity on the fate of carbon," Renew. Sustain. Energy Rev., vol. 104, no. January, pp. 262–280, 2019.
- [5]. H. L. Chum and R. P. Overend, "Biomass and renewable fuels," Fuel Process. Technol., vol. 71, no. 1–3, pp.187–195, 2001.
- [6]. D. Mallick, P. Mahanta, and V. S. Moholkar, "Synergistic Effects in Gasification of Coal/Biomass Blends: Analysis and Review," pp. 473–497, 2018.
- [7]. M. L. Kubacki, A. B. Ross, J. M. Jones, and A. Williams, "Small-scale co-utilisation of coal and biomass," Fuel, vol. 101, pp. 84–89, 2012.
- [8]. G. Lopez, M. Olazar, M. Amutio, J. Bilbao, R. Aguado, and M. Artetxe, "Kinetic study of lignocellulosic biomass oxidative pyrolysis," Fuel, vol. 95, pp. 305–311, 2011.
- [9]. S. Munir, S. S. Daood, W. Nimmo, A. M. Cunliffe, and B. M. Gibbs, "Thermal analysis and devolatilization kinetics of cotton stalk, sugar cane bagasse and shea meal under nitrogen and air atmospheres," Bioresour. Technol., vol. 100, no. 3, pp. 1413–1418, 2009.
- [1]. A. W. Palumbo, C. J. Bartel, J. C. Sorli, and A. W. Weimer, "Characterization of products derived from the high temperature flash pyrolysis of microalgae and rice hulls," Chem. Eng. Sci., vol. 196, no. xxxx, pp. 527–537, 2019.
- [2]. Z. Hu et al., "Thermogravimetric analysis of co-combustion of biomass and biochar," J. Therm. Anal. Calorim., vol. 112, no. 3, pp. 1475–1479, 2012.
- [3]. S. G. Sahu, P. Sarkar, N. Chakraborty, and A. K. Adak, "Thermogravimetric assessment of combustion characteristics of blends of a coal with different biomass chars," Fuel Process. Technol., vol. 91, no. 3, pp.369–378, 2010.
- [4]. D. López-González, M. Fernandez-Lopez, J. L. Valverde, and L. Sanchez-Silva, "Kinetic analysis and thermal characterization of the microalgae combustion process by thermal analysis coupled to mass spectrometry," Appl. Energy, vol. 114, pp. 227–237, 2014.
- [5]. J. Rianza et al., "Combustion of single biomass particles in air and in oxy-fuel conditions," Biomass and Bioenergy, vol. 64, pp. 162–174, 2014.
- [6]. A. Magdziarz and M. Wilk, "Thermogravimetric study of biomass, sewage sludge and coal combustion," Energy Convers. Manag., vol. 75, no. 2013, pp. 425–430, 2013.
- [7]. S. Li, S. Xu, S. Liu, C. Yang, and Q. Lu, "Fast pyrolysis of biomass in free-fall reactor for hydrogen-rich gas," Fuel Process. Technol., vol. 85, no. 8–10, pp. 1201–1211, 2004.
- [8]. Y. El may, M. Jeguirim, S. Dorge, G. Trouvé, and R. Said, "Experimental investigation on gaseous emissions from the combustion of date palm residues in laboratory scale furnace," Bioresour. Technol., vol.131, pp. 94–100, 2013.
- [9]. Y. El may, M. Jeguirim, S. Dorge, G. Trouvé, and R. Said, "Study on the thermal behavior of different date palm residues: Characterization and devolatilization kinetics under inert and oxidative atmospheres," Energy, vol. 44, no. 1, pp. 702–709, 2012.

- [10] A. B. Phadnis and V. V. Deshpande, "Determination of the kinetics and mechanism of a solid state reaction. A simple approach," *Thermochim. Acta*, vol. 62, no. 2–3, pp. 361–367, 1983.
- [11] M. V Gil, D. Casal, C. Pevida, J. J. Pis, and F. Rubiera, "Bioresource Technology Thermal behaviour and kinetics of coal / biomass blends during co-combustion," *Bioresour. Technol.*, vol. 101, no. 14, pp. 5601–5608, 2010.
- [12] V. Dhyani and T. Bhaskar, *Kinetic Analysis of Biomass Pyrolysis*. Elsevier B.V., 2018.
- [13] S. H. Kim, "Investigation of Thermodynamic Parameters in the Thermal Decomposition of Plastic Waste - Waste Lube Oil Compounds," vol. 44, no. 13, pp. 5313–5317, 2010.
- [14] B. Chen, D. Zhou, and L. Zhu, "Transitional adsorption and partition of nonpolar and polar aromatic contaminants by biochars of pine needles with different pyrolytic temperatures," *Environ. Sci. Technol.*, vol. 42, no. 14, pp. 5137–5143, 2008.
- [15] M. Keiluweit, P. S. Nico, and M. G. Johnson, "Dynamic Molecular Structure of Plant Biomass-derived Black Carbon (Biochar)-Supporting Information -," vol. 44, no. 4, pp. 1–19, 2010.
- [16] Q. Wang, G. Wang, J. Zhang, J. Y. Lee, H. Wang, and C. Wang, "Combustion behaviors and kinetics analysis of coal, biomass and plastic," *Thermochim. Acta*, vol. 669, no. June, pp. 140–148, 2018.
- [17] L. T. Vlaev, V. G. Georgieva, and S. D. Genieva, "Products and kinetics of non-isothermal decomposition of vanadium(IV) oxide compounds," *J. Therm. Anal. Calorim.*, vol. 88, no. 3, pp. 805–812, 2007.
- [18] L. Huang et al., "Thermodynamics and kinetics parameters of co-combustion between sewage sludge and water hyacinth in CO<sub>2</sub>/O<sub>2</sub> atmosphere as biomass to solid biofuel," *Bioresour. Technol.*, vol. 218, pp. 631–642, 2016.

HADEY Chaimaa, et. al. "Analysis of the Biomass Behavior in the Combustion Process." *American Journal of Engineering Research (AJER)*, vol. 10(11), 2021, pp. 26-35.